Disulfide Bond Shuffling in Bovine α-Lactalbumin: MD Simulation Confirms Experiment†

Nathan Schmid,‡ Christine Bolliger,‡ Lorna J. Smith,§ and Wilfred F. van Gunsteren*,‡

Laboratory of Physical Chemistry, Swiss Federal Institute of Technology ETH, 8093 Zürich, Switzerland, and Chemistry Research Laboratory, Inorganic Chemistry Laboratory, Department of Chemistry, University of Oxford, South Parks Road, Oxford OX1 3QR, United Kingdom

Received July 17, 2008; Revised Manuscript Received September 12, 2008

ABSTRACT: A simple and straightforward classical molecular dynamics simulation technique is proposed to predict possible disulfide bridge shuffling. Application to bovine α-lactalbumin shows that shuffling can be observed on short simulation time scales and yields results in agreement with experiment.

The protein bovine α-lactalbumin is used extensively as a model system for studying protein structure, stability, and folding (*1*−*3*). A number of recent experimental studies have probed the formation of partially folded or misfolded forms of α-lactalbumin containing non-native disulfide bridges (*4*−*10*). Disulfide scrambling studies performed in the presence of a thiol initiator have identified an isomer, X-αLA-c, which is a predominant folding intermediate (*7, 8*). This isomer contains two native disulfide bridges within the α-helical domain of the protein (6−120, 28−111) but two scrambled disulfide bonds within the *β*-domain of the protein (61−73, 77−91). The non-native disulfide bond 61−73 in the *β*-domain has also been identified in samples of bovine α-lactalbumin heated for a prolonged period of time but without a thiol initiator (*11*). Although the experimental heating period of 2 h at 353 K at pH 7 used in this study is too long to be covered by molecular dynamics (MD) simulation, it is still possible to investigate possible S−S bridge shuffling by computer simulation. To this end, we performed three 20 ns MD simulations, at $T = 298$, 353, and 373 K, of BLA[1] without disulfide bridges in aqueous solution. Since BLA has eight cysteine residues, the molecule could make 28 different S−S bridges. However, considering the distances between Cys residues in the native structure (Figure 1), only residues 61, 73, 77, and 91 are likely candidates for shuffling without a major refolding of the protein. We analyzed the six different pairings of these four residues in a MD simulation and observed the emergence of the non-native 61−73 pair at high temperature, in agreement with experiment.

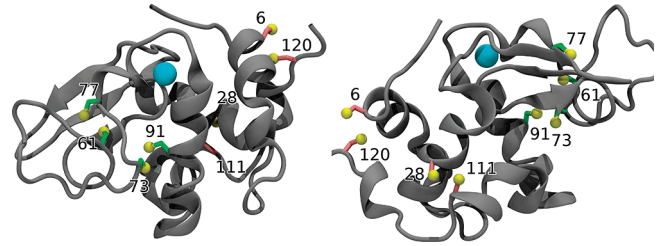

FIGURE 1: Cartoon representation of bovine α-lactalbumin (silver) and the bound Ca^{2+} ion (light blue). The cysteine side chains 61, 73, 77, and 91 of the *β*-domain are shown in green (carbon) and yellow (sulfur), and those of the α-domain (6, 28, 111, and 120) in pink (carbon) and yellow (sulfur).

MATERIALS AND METHODS

Simulation Setup. All simulations were performed using the GROMOS biomolecular simulation software (*12*) and the 53A6 GROMOS force field (*13, 14*). In order to improve sampling of the disulfide bond shuffling all native (6−120, 28−111, 61−77, and 73−91) disulfide bond-length constraints and the corresponding bond angle and dihedral angle potential energy terms were removed from all cysteine residues resulting in eight neutral (no partial charges, unphysical) cysteine residue side chains. Initial coordinates of the protein and the Ca^{2+} ion were taken from the crystal structure deposited in the Protein Data Bank (PDB) with the entry code 1HFZ (*15*). All missing hydrogens were generated by the *gch* GROMOS++ (*12*) program. The protein was solvated in a cubic box containing 9613 simple point charge (SPC) water (*16*) molecules. Periodic boundary conditions were applied. All simulations were initiated with the following equilibration scheme. First, the initial velocities were randomly generated from a Maxwell−Boltzmann distribution at 60 K. All solute atom positions were restrained to their positions in the crystal structure through a harmonic potential energy term with force constant of 2.5×10^4 kJ mol^{-1} nm^{-2}. The system was simulated with these settings for 20 ps. Before three consecutive 20 ps simulations, the temperature was raised by 60 K with the positional restraints being reduced by a factor 10 at each step. Before the next three 20 ps simulations, the position restraints were removed and

† Financial support from the National Center of Competence in Research (NCCR) Structural Biology of the Swiss National Science Foundation (SNSF) is gratefully acknowledged.

* To whom correspondence should be addressed. Phone: +41 44 632 5501. Fax: + 41 44 632 1039. E-mail: wfvgn@igc.phys.chem.ethz.ch.

‡ Swiss Federal Institute of Technology ETH.

§ University of Oxford.

[1] Abbreviations: BLA, bovine α-lactalbumin; MD, molecular dynamics; PDB, Protein Data Bank; rmsd, root mean square deviation; SPC, simple point charge.

10.1021/bi8013455 CCC: $40.75
Published on Web 10/23/2008

the temperature was raised to 298, 353, and 373 K resulting in three starting configurations for the main sampling runs. Next, three 20 ns production simulations were performed. The temperature and atmospheric pressure were kept constant using a weak-coupling approach (*17*) with relaxation times $\tau_T = 0.1$ ps and $\tau_p = 0.5$ ps and an isothermal compressibility of 4.575×10^{-4} (kJ mol^{-1} nm^{-3})$^{-1}$. Nonbonded interactions were calculated using a triple-range cutoff scheme. The interactions within a cutoff distance of 0.8 nm were calculated at every step from a pair list which was updated every fifth time step. At this point, interactions between atoms (of charge groups) within 1.4 nm were also calculated and were kept constant between updates. To account for the influence of the dielectric medium outside the cutoff sphere of 1.4 nm, a reaction-field force based on a relative dielectric permittivity ε of 61 (*18*) was added.

Analysis. The atom-positional root-mean-square deviation (rmsd) between the indicated atoms of two structures was calculated after superposition of the indicated atoms. Secondary structure of the protein was assigned according to the rules defined by Kabsch and Sander's DSSP (*19*). The presence of a hydrogen bond was determined by geometric criteria. If the hydrogen-acceptor distance was less than 0.25 nm and the donor−hydrogen−acceptor angle was at least 135°, the hydrogen bond was considered to be present. Disulfide bridges were identified with a sulfur−sulfur distance of less than 0.5 nm.

Software and Hardware. All simulation and energy minimization computations were carried out using MD++ 0.2.3 of the GROMOS05 package (*12*). For analysis, GROMOS++ 0.2.4 (*12*) was used. Additional analysis, conversion, and batch programs were written in Perl. Visualization was done with the Visual Molecular Dynamics (VMD) (*20*) software.

RESULTS AND DISCUSSION

As initial structures for the simulations, the crystal structure of BLA (123 residues) was taken and all disulfide bridges were artificially broken. The native structure of BLA contains several secondary structure elements, namely α-helices (4−13, 23−34, 85−99, and 104−111) and 3_{10}-helices (76−81 and 115−119) and a β-sheet (42−57), a calcium ion binding site, and several disulfide bridges (Figure 1). The side chains of the cysteine residues that are likely to be involved in disulfide bridge shuffling (61, 73, 77, and 91) are highlighted.

Three 20 ns long simulations at temperatures of 298, 353, and 373 K were carried out. The time series of atom-positional root-mean-square deviations of the backbone atoms from the initial structure are shown in Figure 2. One can easily see that the structure is conserved to a large extent when simulating BLA with broken disulfide bridges at 298 K. The rmsd is converging to a comparatively low value of 0.38 nm. For higher temperatures the situation is different: there are large deviations from the initial structure. This is an indication that the backbone of the protein is deformed in the course of the simulation. The radius of gyration analysis (Figure 3) contains strong indications that the protein is in a partially folded state at higher temperatures. Only at 373 K the tertiary globular structure is lost after 5 ns. Surprisingly, after an additional 5 ns the globular shape is reformed and remains stable for another 10 ns.

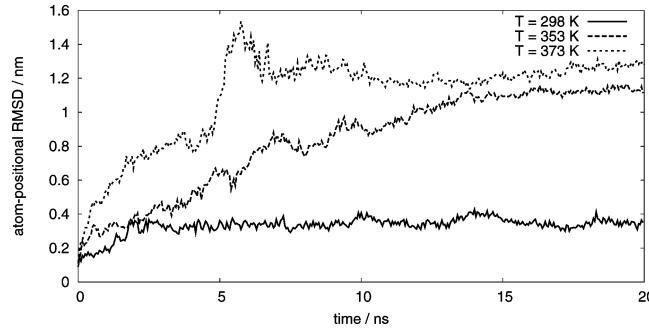

FIGURE 2: Time series of the atom-positional backbone rmsd of the MD trajectory structures from the initial X-ray structure for the three different temperature simulations (298 K red/solid, 353 K green/dashed, 373 K blue/dotted).

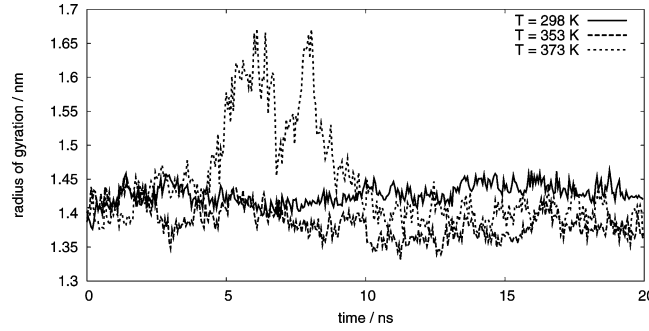

FIGURE 3: Time series of the radius of gyration of backbone atoms for the MD trajectory structures at three different temperatures (298 K red/solid, 353 K green/dashed, 373 K blue/dotted).

Table 1: Population of Hydrogen Bonds between Backbone NH and CO of the Indicated Residues[a]

hydrogen bond NH−CO	temperature 298 K	353 K	373 K	hydrogen bond NH−CO	temperature 298 K	353 K	373 K
Helix 1				**3_{10}-Helix 1**			
8−4	57	80	69	79−76	4	1	1
9−5	69	85	73	80−77	7	2	1
10−6	77	78	30	81−78	18	1	1
12−8	15	68	23	**Helix 3**			
13−10	3	2	2	89−85	7	14	24
Helix 2				90−86	45	15	18
27−23	96	71	67	91−87	95	29	33
28−24	98	80	19	92−88	91	30	35
29−25	49	82	15	93−89	92	33	36
30−26	83	47	14	94−90	88	32	66
31−27	8	52	7	95−91	64	25	65
32−28	13	41	20	96−92	45	8	34
33−29	97	31	14	97−93	30	2	1
34−30	54	17	43	98−94	17	1	1
Sheet 1				99−95	32	20	1
42−49	90	17	30	**Helix 4**			
44−47	92	11	4	107−104	0	0	6
49−42	97	17	21	108−104	2	0	17
51−40	94	11	31	109−105	47	62	28
54−51	95	41	32	110−106	5	65	7
55−50	1	1	19	111−107	2	19	0
57−48	85	25	8	**3_{10}-Helix 2**			
				118−115	28	17	0
				119−116	10	7	0

[a] Values are given in percent (%) occurrence during the 20 ns of the simulations. Hydrogen bonds were defined using geometrical criteria: if the H−O distance was less than 0.25 nm and the N−H−O angle was at least 135°, the hydrogen bond was considered to be present.

The backbone hydrogen bonds of secondary structural elements (Table 1) and the secondary structure (Figure 4) were analyzed to see whether the protein only loses its

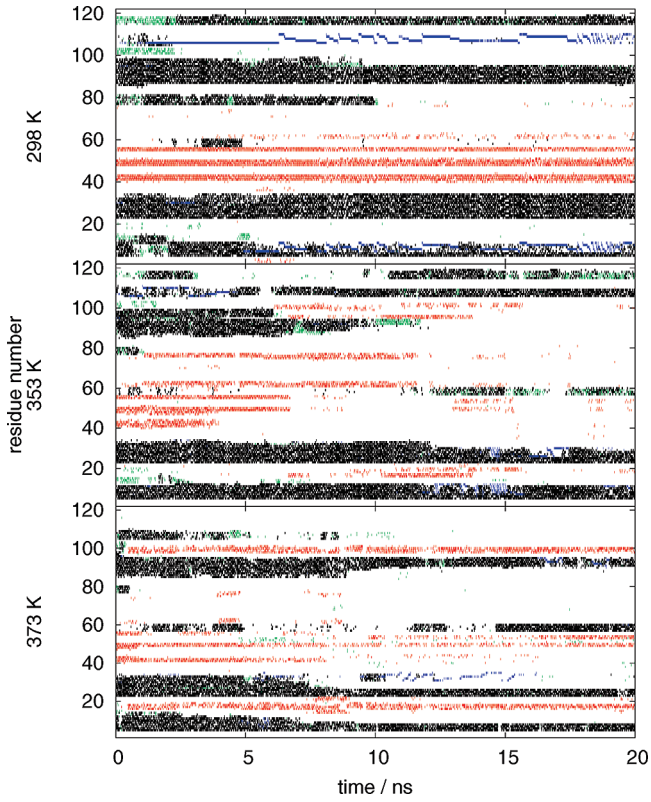

FIGURE 4: Time series of secondary structure elements (3_{10}-helix (green), α-helix (black), π-helix (blue), and β-strand (red)) per residue for the three different temperature simulations.

compact fold but keeps its secondary structure. Such characteristics would be similar to those in the molten globule state of α-lactalbumin which has been observed in previous experiments and MD simulations (*1*−*3*, *21*). The populations of hydrogen bonds of the secondary structural elements are given in Table 1. At 298 K, all secondary structure elements with the exception of the 3_{10}-helices and helix 4 can be considered as stable. Helix 4 is lost during the simulation and refolds into a sort of π-helix (Figure 4). It is worth mentioning that the β-sheet and helix 3 are stable, although the disulfide bridges were broken. This can be taken as a hint that disulfide bridge 73−91 has an ancillary role in the stability of these secondary structure elements. The calcium ion remains bound in its binding pocket during the whole 20 ns of the simulation. At higher temperatures (353 and 373 K) the general stability of the helices is highly reduced. First, in both simulations the large helix 3 is almost completely lost. Second, the β-sheet shows a surprisingly high stability: at 353 K the sheet's secondary structure is lost and reformed multiple times. Last, already after 5 ns the Ca^{2+} ion drifts away from the binding pocket and moves freely through the simulation box (data not shown). The loss of calcium from the structure is interesting as experimental studies show that α-lactalbumin does not bind calcium in the absence of the β-domain disulfide bonds (*5*, *9*).

The native disulfide bridges (6−120, 28−111, 61−77, 73−91) and the non-native disulfide bridges of the α-domain (6−28, 6−111, 28−120, 111−120) and of the β-domain (61−73, 61−91, 73−77, 77−91) were analyzed in more detail by monitoring the S−S distance of the corresponding cysteine residues (Figure 5). The native disulfide S−S distances are in general short throughout the 298 K simulation reflecting the fact that the protein structure remains folded. An exception is the 6−120 distance which varies considerably even at 298 K. This agrees with experimental studies that have identified that this disulfide bridge shows superreactivity arising from geometrical strain imposed by the native fold of the protein (10). In the native protein this 6−120 disulfide is readily reduced and the resultant three-

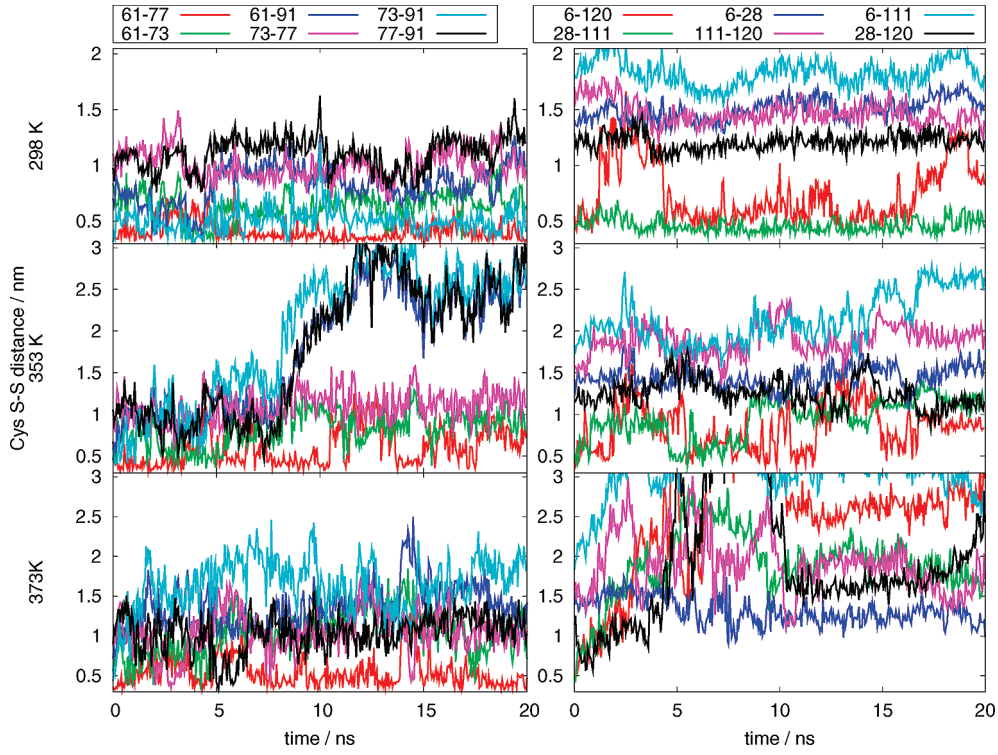

FIGURE 5: Time series of sulfur−sulfur distances for the four cysteine residues (61, 73, 77, and 91) of the β-domain (left panel) and for the four cysteine residues (6, 28, 111, and 120) of the α-domain (right panel) prone to shuffling.

disulfide species adopts a native-like structure when calcium is bound (10). At higher temperatures all the native disulfide S−S distances show larger fluctuations in the simulations. Indeed at 373 K only the 61−77 distance remains short throughout most of the simulation. This reflects unfolding of the protein at these temperatures: the secondary structure elements drift away from each other as they are not linked by covalent S−S bridges in these simulations.

The various possible disulfide distances are shown in Figure 5. The non-native ones of the α-domain all stay beyond 1 nm at any of the three temperatures, which is not surprising considering their distances in the native structure (Figure 1). The β-domain shows a different picture. At 298 K the ranking from shortest to longest of the six distances is 61−77, 73−91, 61−73, 61−91, 73−77, 77−91, the two native disulfide pairs being the shortest ones. At 353 K the ranking is changed to 61−77, 61−73, 73−77, 77−91, 61−91, 73−91, where the latter three show very large distances. At 373 K the ranking is essentially the same, although the longtest three distances are lower. This indicates that at higher temperature the native 73−91 disulfide bridge is broken. Considering the location of the four residues 61, 73, 77 and 91 with respect to the protein's secondary structure, the first three are in a loop, whereas 91 is part of helix 3. This may explain that at higher temperatures the first three may make disulfide bridges between each other while 91 is less likely to be involved. Of the three distances between residues 61, 73, and 77, the native one 61−77 is the shortest, but the other two also show occasionally low values. The 61−73 bridge could form in all three simulations. This is the linkage that can be obtained by incubating the protein at higher temperature. The 61−73 distance fluctuates through the simulations but short approaches are seen within 4 ns of the simulation at 298 K. Here the protein structure is very native-like and the conformation may resemble the predominant folding intermediate, X-αLA-c, seen experimentally (7,8). All the helices persist in the structure at this point in the simulation, which agrees with the observation that the far-UV CD spectrum of X-αLA-c retains a substantial amount of α-helical secondary structure (22). The fact that the 61−73 bridge is also observed at lower temperature in our unphysical model can be taken as a hint that higher temperatures or a thiol initiator is needed to break the native bridge and to enhance the probability of collision of the sulfur atoms of residues 61 and 73. In our model, we removed charge repulsion between the sulfur atoms in order to allow sampling of this event on a much shorter time scale. With the help of this model we can observe shuffling of the 61−73 and 61−77 disulfide bridges.

CONCLUSIONS

We showed by our simulations that S−S shuffling can be observed in classical MD simulations even on short time scales of several nanoseconds. We introduced a simple model for S−S shuffling by removing charge repulsion from the sulfur atoms and showed that the model can be used to gain qualitative insight into the mechanisms of protein folding and S−S bridge stability. In the case of BLA we were able to observe the formation of the non-native S−S bridge 61−73 which is in agreement with the experimental observations.

REFERENCES

1. Ptitsyn, O. B. (1995) Molten globule and protein folding. *Adv. Protein Chem. 47*, 83–229.
2. Kuwajima, K. (1996) The molten globule state of alpha-lactalbumin. *FASEB J. 10*, 102–109.
3. Permyakov, E. A., and Berliner, L. J. (2000) alpha-Lactalbumin: structure and function. *FEBS Lett. 473*, 269–274.
4. Peng, Z. Y., Wu, L. C., and Kim, P. S. (1995) Local structural preferences in the alpha-lactalbumin molten globule. *Biochemistry 34*, 3248–3252.
5. Wu, L. C., Peng, B. A., and Peng, Z. Y. (1996) Disulfide determinants of calcium-induced packing in alpha-Lactalbumin. *Biochemistry 35*, 859–863.
6. Chakraborty, S., and Peng, Z. Y. (2000) Hierarchical unfolding of the alpha-lactalbumin molten globule: Presence of a compact intermediate without a unique tertiary fold. *J. Mol. Biol. 298*, 1–6.
7. Chang, J. Y. (2001) The structure of denatured alpha-lactalbumin elucidated by the technique of disulfide scrambling—Fractionation of conformational isomers of alpha-lactalbumin. *J. Biol. Chem. 276*, 9705–9712.
8. Chang, J. Y. (2002) The folding pathway of alpha-lactalbumin elucidated by the technique of disulfide scrambling - Isolation of on-pathway and off-pathway intermediates. *J. Biol. Chem. 277*, 120–126.
9. Last, A. M., Schulman, B. A., Robinson, C. V., and Redfield, C. (2001) Probing subtle differences in the hydrogen exchange behavior of variants of the human alpha-lactalbumin molten globule using mass spectrometry. *J. Mol. Biol. 311*, 909–919.
10. Kuwajima, K., Ikeguchi, M., Sugawara, T., Hiraoka, Y., and Sugai, S. (1990) Kinetics of disulfide bond reduction in alpha-lactalbumin by dithiothreitol and molecularbasis of superreactivity of the cys6-cys120 disulfide bond. *Biochemistry 29*, 8240–8249.
11. Wijesinha-Bettoni, R., Gao, C., Jenkins, J. A., Mackie, A. R., Wilde, P. J., Mills, E. N. C., and Smith, L. J. (2007) Heat Treatment of Bovine α-Lactalbumin Results in Partially Folded, Disulfide Bond Shuffled State with Enhanced Surface Activity. *Biochemistry 46*, 9774–9784.
12. Christen, M., Hüenenberger, P. H., Bakowies, D., Baron, R., Büergi, R., Geerke, D. P., Heinz, T. N., Kastenholz, M. A., Kräeutler, V., Oostenbrink, C., Peter, C., Trzesniak, D., and van Gunsteren, W. F. (2005) The GROMOS software for biomolecular simulation: GROMOS05. *J. Comput. Chem. 26*, 1719–1751.
13. Oostenbrink, C., Villa, A., Mark, A. E., and van Gunsteren, W. F. (2004) A biomolecular force field based on the free enthalpy of hydration and solvation: the GROMOS force-field parameter sets 53A5 and 53A6. *J. Comput. Chem. 25*, 1656–1676.
14. Oostenbrink, C., Soares, T. A., van der Vegt, N. F. A., and van Gunsteren, W. F. (2005) Validation of the 53A6 GROMOS force field. *Eur. Biophys. J. 34*, 273–284.
15. Pike, A. C., Brew, K., and Acharya, K. R. (1996) Crystal structures of guinea-pig, goat and bovine alpha-lactalbumin highlight the enhanced conformational flexibility of regions that are significant for its action in lactose synthase. *Structure 4*, 691–703.
16. Berendsen, H. J. C., Postma, J. P. M., van Gunsteren, W. F., and Hermans, J. (1981) in *Intermolecular Forces* (Pullmann B., et al., Eds.) pp 331−342, Reidel, Dordrecht, The Netherlands.
17. Berendsen, H. J. C., Postma, J. P. M., van Gunsteren, W. F., DiNola, A., and Haak, J. R. (1984) Molecular dynamics with coupling to an external bath. *J. Chem. Phys. 81*, 3684–3690.
18. Heinz, T. N., van Gunsteren, W. F., and Huenenberger, P. H. (2001) Comparison of four methods to compute the dielectric permittivity of liquids from molecular dynamics simulations. *J. Chem. Phys. 115*, 1125–1135.
19. Kabsch, W., and Sander, C. (1983) Dictionary of protein secondary structure: Pattern recognition of hydrogen-bonded and geometrical features. *Biopolymers 22*, 2577–2637.
20. Humphrey, W., Dalke, A., and Schulten, K. (1996) VMD - Visual Molecular Dynamics. *J. Mol. Graph. 14*, 33–38.
21. Schäefer, H., Smith, L. J., Mark, A. E., and van Gunsteren, W. F. (2002) Entropy Calculations of the Molten Globule State of a Protein: Side-Chain Entropies of alpha-Lactalbumin. *Proteins 46*, 215–224.
22. Chang, J. Y., Bulyclev, A., and Li, L. (2000) A stabilized molten globule protein. *FEBS Lett. 487*, 298–300.

BI8013455